Crystallization Process of $Fe_{75}Co_5Zr_{10}B_{10}$ Amorphous Alloy

Y.M. Sun, B. Zuo, D. Wang, X.C. Meng, J. Liu, L.L. Wang and Z. Hua*
Key Laboratory of Functional Materials Physics and Chemistry of the Ministry of Education
Jilin Normal University, Siping 136000, Jilin, China

(Received December 21, 2012; in final form May 5, 2013)

$Fe_{75}Co_5Zr_{10}B_{10}$ amorphous alloy prepared by melt-spinning was annealed at various temperatures. The thermal property and microstructures were investigated by differential thermal analysis, X-ray diffraction, and transmission electron microscopy. The crystallization process of $Fe_{75}Co_5Zr_{10}B_{10}$ amorphous alloy is complex. The α-Fe phase precipitates from the amorphous matrix in the initial stage of crystallization. The α-Mn type (χ) phase precipitates at 570 °C, but transforms to α-Fe phase and the Laves C14(λ) phase at higher temperature. In the final stage of crystallization, Fe_3Zr, Fe_2Zr, and unknown phases are observed and the λ-phase disappears. The α-Fe phase preferentially nucleates after annealing at 530 °C for 10 min and the χ-phase preferentially nucleates after annealing at 600 °C for 10 min. The nucleation barrier of χ-phase is larger than that of α-Fe phase. The local structure of χ-phase is more similar to amorphous phase.

DOI: 10.12693/APhysPolA.124.685
PACS: 61.43.Dq, 64.60.My

1. Introduction

Fe-based nanocrystalline soft magnetic alloys have been extensively investigated over the past several decades [1–8]. The study on crystallization process is one of the key research contents of Fe-based amorphous alloys. Many special metastable phases formed during the crystallization process have attracted continuous interest in recent years. The cubic quasiperiodic (CQ), nanocrystalline CQ (NCQ), Laves C14(λ), α-Mn type (χ) and hexagonal (H) phases were observed in the primary crystallization processes of Fe–Si–B–Nb alloys [8–10]. $Fe_{23}B_6$ phase was observed in other Fe(Co)–Si–B–Nb alloys [5, 11]. For Fe–M–B (M = Zr, Nb) alloys, α-Mn type [6, 12] and $Fe_{23}B_6$ [13–15] metastable phases were observed in the primary crystallization processes. So many kinds of metastable phases form as primary crystallization phases. The formation of specific phases and their fast nucleation are associated with three aspects: similarity between local structures of the metastable and amorphous phases, high activation barriers for long range rearrangement necessary for formation of primary phases in stable supercooled liquid and surface energy [8].

In this paper, the α-Mn type (χ) and Laves C14(λ) metastable phases were observed during the crystallization process of $Fe_{75}Co_5Zr_{10}B_{10}$ alloy. The phase transformation was studied.

2. Experimental details

$Fe_{75}Co_5Zr_{10}B_{10}$ amorphous alloy ribbon was prepared by melt-spinning and annealed at 530, 570, 600, 630, 680, and 730 °C for different annealing times. Structural characterizations of samples were examined by X-ray diffraction (XRD, D/max 2500/PC, Cu K_α, $\lambda = 1.5406$ Å) and transmission electron microscopy (TEM, JEM-2100E). The thermal analysis was investigated by differential thermal analysis (DTA, TG/DTA-6300) at a heating rate of 20 K/min.

3. Results and discussion

XRD patterns of $Fe_{75}Co_5Zr_{10}B_{10}$ alloy corresponding to different annealing temperatures for 40 min are shown in Fig. 1. No crystalline peaks are detected in the XRD,

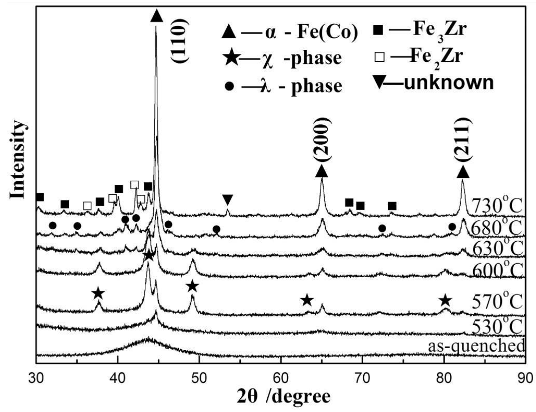

Fig. 1. XRD patterns of $Fe_{75}Co_5Zr_{10}B_{10}$ alloys corresponding to different annealing temperatures for 40 min.

which indicates that the alloy as-quenched forms amorphous. After annealing at 530 °C, only the α-Fe phase precipitates from the amorphous matrix. At 570 °C, the α-Mn type (χ) phase also precipitates in addition to α-Fe phase. Further increase of annealing temperature leads to the disappearance of χ-phase, the growth of α-Fe volume fraction, and the formation of Laves C14(λ) phase.

*corresponding author; e-mail: huazhong196110@163.com

The χ-phase is metastable and transforms to α-Fe phase and λ-phase. The λ-phase is also metastable and disappears at higher temperature. The Fe_3Zr, Fe_2Zr, and unknown phases are observed in the final stage of crystallization, but it is difficult to judge which phase is transformed by λ-phase.

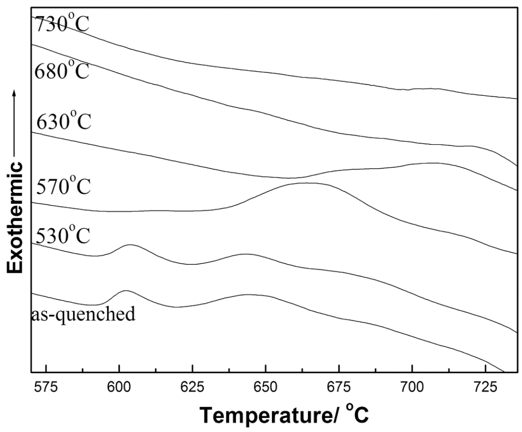

Fig. 2. DTA traces of $Fe_{75}Co_5Zr_{10}B_{10}$ alloys as-quenched and annealed at different temperatures for 40 min.

TABLE

The characteristic crystallization temperatures determined from all DTA curves.

	T_{p1} [K]	T_{p2} [K]	T_{p3} [K]
as-quenched	601.0	646.2	685.3
530 °C	603.9	643.2	682.4
570 °C	–	665.3	714.0
630 °C	–	674.4	711.8
680 °C	–	–	723.2
730 °C	–	–	–

Figure 2 shows the DTA traces of $Fe_{75}Co_5Zr_{10}B_{10}$ alloys as-quenched and after annealing. The characteristic crystallization temperatures determined from all DTA curves are shown in Table. There are three exothermic peaks in the DTA trace of the alloy as-quenched. There is little change in the DTA trace of the alloy annealed at 530 °C. For the alloy annealed at 570 °C, the first exothermic peak (T_{p1}) disappears and the second exothermic peak (T_{p2}) shifts obviously to a higher temperature region, which indicates that the first stage of crystallization is complete. The first exothermal peak should correspond to the formations of α-Fe phase and χ-phase. For the alloy annealed at 680 °C, only a little peak at high temperature region is observed, which indicates that the second stage of crystallization is complete. The second exothermal peak corresponds to the transformation of χ-phase. For the alloy annealed at 730 °C, no peak is observed, indicating that the crystallization is complete. The third exothermal peak (T_{p3}) corresponds to the transformation of λ-phase, and the precipitations of Fe_3Zr, Fe_2Zr, and unknown phases.

Figure 3 shows the TEM image and the corresponding selected-area electron diffraction pattern of $Fe_{75}Co_5Zr_{10}B_{10}$ alloy annealed at 570 °C for 40 min. The nanocrystals surrounded by a residual amorphous matrix are irregularly shaped. Polycrystalline electron diffraction pattern shows the evidence for α-Fe and α-Mn type phases.

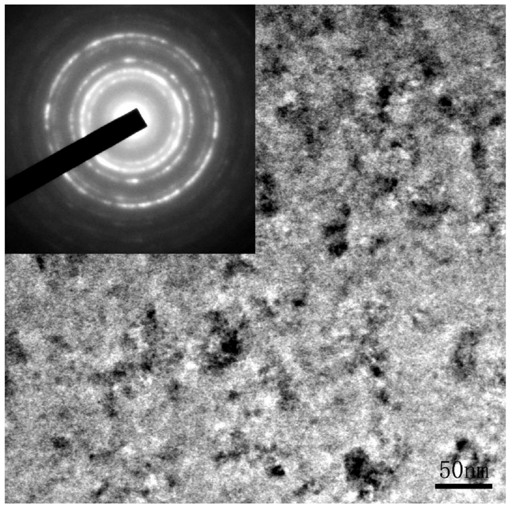

Fig. 3. TEM image and the corresponding selected-area electron diffraction pattern of $Fe_{75}Co_5Zr_{10}B_{10}$ alloys annealed at 570 °C for 40 min.

XRD patterns of $Fe_{75}Co_5Zr_{10}B_{10}$ alloys corresponding to 530, 600, and 630 °C for different annealing times are shown in Fig. 4a–c. The α-Fe phase forms in the alloy annealed at 530 °C for 10 min (Fig. 4a). When annealing time reaches 90 min, the χ-phase precipitates in addition to α-Fe phase. Both the intensity of α-Fe and χ-phase diffraction peaks increase with increasing annealing time. The χ-phase and very little α-Fe phase precipitate in the alloy annealed at 600 °C for 10 min (Fig. 4b). With increasing annealing time, the diffraction intensity of χ-phase increases firstly and then decreases. The intensity of α-Fe diffraction peak increases continuously. The χ-phase transforms to α-Fe phase. The χ-phase and α-Fe phase are observed in the alloy annealed at 630 °C for 10 min (Fig. 4c). With increasing annealing time, the volume fraction of χ-phase decreases with increasing annealing time. The λ-phase is observed in the alloy annealed at 630 °C for 40 min. Further increase of annealing time leads to the disappearance of χ-phase. Only α-Fe phase and λ-phase are observed in the alloy annealed at 630 °C for 180 min.

The crystallization process consists of two major events: nucleation and crystal growth. The formation of new phases begins with the process of nucleation [16]. After annealing at 530 °C for 10 min, α-Fe phase preferentially nucleates. When increasing annealing time or temperature, χ-phase precipitates. It indicates that nu-

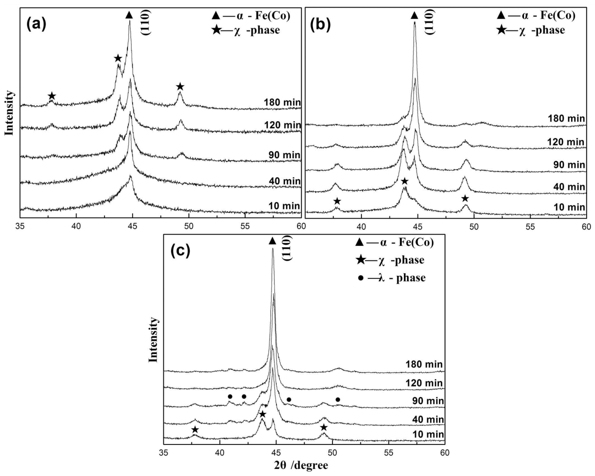

Fig. 4. XRD patterns of $Fe_{75}Co_5Zr_{10}B_{10}$ alloys corresponding to 530 (a), 600 (b), and 630 °C (c) for different annealing times.

cleation barrier of χ-phase is larger than that of α-Fe phase. Moreover, χ-phase preferentially nucleates after annealing at 600 °C for 10 min. It should be that the local structure of χ-phase is more similar to amorphous phase. If thermal energy provided by heat treatment overcomes the nucleation barrier of χ-phase, χ-phase preferentially nucleates rather than α-Fe phase. The χ-phase is metastable and transforms to α-Fe phase with increasing annealing time at 600 °C. When thermal energy provided by heat treatment overcomes the nucleation barrier of λ-phase, χ-phase not only transforms to α-Fe phase but also λ-phase, which is observed in the alloy annealed at 630 °C for 40 min.

4. Conclusions

(1) $Fe_{75}Co_5Zr_{10}B_{10}$ alloy as-quenched forms amorphous. After annealing at 530 °C for 40 min, only α-Fe phase precipitates from the amorphous matrix. The χ-phase and λ-phase are metastable, which are observed at 570 and 630 °C for 40 min, respectively. With increasing annealing temperature, χ-phase transforms to α-Fe phase and λ-phase. The Fe_3Zr, Fe_2Zr, and unknown phases are observed and the λ-phase disappears in the final stage of crystallization.

(2) There are three exothermic peaks in the DTA trace of the alloy as-quenched. The first exothermal peak corresponds to the formations of α-Fe phase and χ-phase. The second exothermal peak corresponds to the transformation of χ-phase into α-Fe phase and λ-phase. The third exothermal peak corresponds to the transformation of λ-phase, and the precipitations of Fe_3Zr, Fe_2Zr, and unknown phases. It is difficult to judge which phase is transformed by λ-phase.

(3) The α-Fe phase preferentially nucleates after annealing at 530 °C for 10 min and the χ-phase preferentially nucleates after annealing at 600 °C for 10 min. The nucleation barrier of χ-phase is larger than that of α-Fe phase. The local structure of χ-phase is more similar to amorphous phase.

Acknowledgments

This work was funded by Science and Technology Development Project of Jilin Province (No. 201105083), Science and Technology Studying Project of "12th five-year" Office of Education of Jilin Province (No. 2011-158) and Graduate Innovative Research Programs of Jilin Normal University (No. 201103).

References

[1] B. Movahedi, M.H. Enayati, C.C. Wong, *Mater. Lett.* **64**, 1055 (2010).

[2] Y. Hu, L. Liu, K.C. Chan, M.X. Pan, W.H. Wang, *Mater. Lett.* **60**, 1080 (2006).

[3] Y.M. Sun, W.Q. Yu, Z. Hua, *Acta Phys. Pol. A* **119**, 374 (2011).

[4] Y. Sun, L. Zhong, X.F. Bi, *Scr. Mater.* **60**, 814 (2009).

[5] Y.R. Zhang, R.V. Ramanujan, *J. Alloys Comp.* **403**, 197 (2005).

[6] T. Nagase, Y. Umakoshi, *Iron Steel Instit. Jpn. Int.* **46**, 1371 (2006).

[7] J.S. Blázquez, V. Franco, A. Conde, *J. Phys., Condens. Matter* **14**, 11717 (2002).

[8] I.V. Lyasotsky, N.B. Dyakonova, D.L. Dyakonov, E.N. Vlasova, M.Yu. Jazvitsky, *Rev. Adv. Mater. Sci.* **18**, 695 (2008).

[9] I.V. Lyasotskii, N.B. Dyakonova, E.N. Vlasova, D.L. Dyakonov, M.Yu. Yazvitskii, *Phys. Status Solidi A* **203**, 259 (2006).

[10] I.V. Lyasotskii, N.B. Dyakonova, E.N. Vlasova, D.L. Dyakonov, B.V. Molotilov, *Bull. Russ. Acad. Sci. Phys.* **65**, 1549 (2001).

[11] A. Hirata, Y. Hirotsu, K. Amiya, N. Nishiyama, A. Inoue, *Intermetallics* **16**, 491 (2008).

[12] W.Q. Yu, Y.M. Sun, Z. Hua, *Appl. Surf. Sci.* **257**, 9733 (2011).

[13] M. Imafuku, S. Sato, H. Koshiba, E. Matsubara, A. Inoue, *Mater. Trans. Jpn. Inst. Metals* **41**, 1526 (2000).

[14] M. Imafuku, S. Sato, H. Koshiba, E. Matsubara, A. Inoue, *Scr. Mater.* **44**, 2369 (2001).

[15] A. Hirata, Y. Hirotsu, E. Matsubara, *Intermetallics* **17**, 796 (2009).

[16] D. Kashchiev, *Nucleation: Basic Theory with Applications*, Butterworth-Heinemann, Oxford 2000.